

RCC calculation of electric dipole polarizability and correlation energy of Cn, Nh⁺ and Og: Correlation effects from lighter to superheavy elements

Ravi Kumar,¹ S. Chattopadhyay,² D. Angom,^{3,4} and B. K. Mani^{1,*}

¹*Department of Physics, Indian Institute of Technology, Hauz Khas, New Delhi 110016, India*

²*Department of Physics, Kansas State University, Manhattan, Kansas 66506, USA*

³*Department of Physics, Manipur University, Canchipur 795003, Manipur, India*

⁴*Physical Research Laboratory, Ahmedabad - 380009, Gujarat, India*

We employ a fully relativistic coupled-cluster theory to calculate the ground-state electric dipole polarizability and electron correlation energy of superheavy elements Cn, Nh⁺ and Og. To assess the trend of electron correlation as function of Z , we also calculate the correlation energies for three lighter homologs—Zn, Cd and Hg; Ga⁺, In⁺ and Tl⁺; Kr, Xe and Rn—for each superheavy elements. The relativistic effects and quantum electro-dynamical corrections are included using the Dirac-Coulomb-Breit Hamiltonian with the corrections from the Uehling potential and the self-energy. The effects of triple excitations are considered perturbatively in the theory. Furthermore, large bases are used to test the convergence of results. Our recommended values of polarizability are in good agreement with previous theoretical results for all SHEs. From our calculations we find that the dominant contribution to polarizability is from the valence electrons in all superheavy elements. Except for Cn and Og, we observe a decreasing contribution from lighter to superheavy elements from the Breit interaction. For the corrections from the vacuum polarization and self-energy, we observe a trend of increasing contributions with Z . From energy calculations, we find that the second-order many-body perturbation theory overestimates the electron correlation energy for all the elements considered in this work.

I. INTRODUCTION

The study of superheavy elements (SHEs) is a multidisciplinary research area which provides a roadmap to investigate and understand several properties related to physics and chemistry [1–6]. There is however a lack of experimental data on atomic properties of SHEs due to various challenges, such as low production rate, short half-lives of elements and the lack of the state of the art one-atom-at-a-time experimental facility, associated with atomic experiments [1, 7, 8]. Moreover, the properties of SHEs can not be predicted based on lighter homologs, as they often differ due to relativistic effects in SHEs [5]. In such cases, the theoretical investigations of physical and chemical properties provide an important insight to the properties of SHEs. Moreover, the benchmark data on these properties from accurate theoretical predications is important for future experiments. Calculating accurate properties of SHEs is, however, a difficult task. The reason for this could be attributed to the competing nature of the relativistic and correlation effects in these systems. For a reliable prediction of the properties of SHEs both of these effects should be incorporated at the highest level of accuracy. In addition, large basis sets should be used to obtain the converged properties results.

The electric dipole polarizability, α , of an atom or ion is a key parameter which used to probe several fundamental as well as technologically relevant properties in atoms and ions [9–14]. The α for SHEs Cn and Og has been calculated in previous works, Refs. [15–18] and [16, 17, 19, 20], respectively. Though most of these results are using the CCSD(T), there is a large variation in the reported values for both Cn and Og. For example, the value of α reported in CCSD(T) calculation

[20] is $\approx 25\%$ larger than the similar calculation [19]. The reason for this can, perhaps, be attributed to the complex nature of the electron correlation and relativistic effects in these systems. The other point to be mentioned here is that, the basis used in these calculations are not large. Moreover, the inclusion of the contributions from the Breit interaction and QED corrections is crucial to obtain the accurate and reliable values of α for SHEs.

In this work, we employ a fully relativistic coupled cluster (RCC) theory based method to calculate the electric dipole polarizability and the electron correlation energy of superheavy elements Cn, Nh⁺ and Og. RCC is one of the most powerful many-body theories for atomic structure calculations as it accounts for the electron correlation to all-orders of residual Coulomb interaction. We have used this to calculate the many-electron wavefunction and the electron correlation energy. The effect of external electric field, in the case of α , is accounted using the perturbed relativistic coupled-cluster (PRCC) theory [21–25]. One of the key merits of PRCC in the properties calculation is that it does not employ the sum-over-state [26, 27] approach to incorporate the effects of a perturbation. The summation over all the possible intermediate states is subsumed in the perturbed cluster operators. The leading order relativistic effects are accounted using the four component Dirac-Coulomb-Breit no-virtual-pair Hamiltonian [28]. And, the effects of Breit, QED and triples excitations in coupled-cluster are computed using the implementations in our previous works [21–24].

To assess the trend of various electron correlation effects from lighter to SHEs, we also calculate the correlation energy and the contributions from the Breit and QED corrections to α for three lighter homologs in each SHEs: Zn, Cd and Hg in group-12; Ga⁺, In⁺ and Tl⁺ in group-13; and Kr, Xe, and Rn in group-18. In this work, however, we do not report the values of α for these lighter homologs as these have been already reported in our previous works [21, 24, 25]. Here, our main

* bkmani@physics.iitd.ac.in

focus is to get deeper insight of various correlation effects as a function Z in each of these SHEs. More precisely, we aimed to: accurately calculate the value of α and correlation energy of SHEs Cn, Nh^+ and Og using RCC and test the convergence of results with very large basis; study the electron correlation in α for SHEs and assess the trend from lighter to SHEs; and examine in detail the contributions from the Breit and QED corrections to α for SHEs elements and get a deeper insight to the trend of contributions from lighter homologs to SHEs.

The remaining part of the paper is organized into five sections. In Sec. II we provide a brief description of the method used in the polarizability calculation. In Sec. III we provide the calculational details such as the single-electron basis and computational challenges associated with polarizability calculation of SHEs. In Sec. IV we analyze and discuss the results from our calculations. The theoretical uncertainty in our calculation is discussed in Sec. V. Unless stated otherwise, all the results and equations presented in this paper are in atomic units ($\hbar = m_e = e = 1/4\pi\epsilon_0 = 1$)

II. METHOD OF CALCULATION

The ground state wavefunction of an N -electron atom or ion in relativistic coupled-cluster (RCC) theory is

$$|\Psi_0\rangle = e^{T^{(0)}}|\Phi_0\rangle, \quad (1)$$

$$\langle\Phi_a^p|H_N + [H_N, T^{(0)}] + \frac{1}{2!} [[H_N, T^{(0)}], T^{(0)}] + \frac{1}{3!} [[[[H_N, T^{(0)}], T^{(0)}], T^{(0)}], T^{(0)}]|\Phi_0\rangle = 0, \quad (3a)$$

$$\langle\Phi_{ab}^{pq}|H_N + \frac{1}{2!} [[H_N, T^{(0)}], T^{(0)}] + \frac{1}{3!} [[[[H_N, T^{(0)}], T^{(0)}], T^{(0)}], T^{(0)}] + \frac{1}{4!} [[[[[[H_N, T^{(0)}], T^{(0)}], T^{(0)}], T^{(0)}], T^{(0)}], T^{(0)}]|\Phi_0\rangle = 0. \quad (3b)$$

Here, the states $|\Phi_a^p\rangle$ and $|\Phi_{ab}^{pq}\rangle$ are the singly- and doubly-excited determinants obtained by replacing *one* and *two* electrons from the core orbitals in $|\Phi_0\rangle$ with virtual orbitals, respectively. And, $H_N = H^{\text{DCB}} - \langle\Phi_0|H^{\text{DCB}}|\Phi_0\rangle$ is the normal-ordered Hamiltonian.

In the presence of an external electric field, \mathbf{E}_{ext} , the ground state wavefunction $|\Psi_0\rangle$ is modified due to interaction between induced electric dipole moment \mathbf{D} of the atom and \mathbf{E}_{ext} . We call the modified wavefunction as the perturbed wavefunction, which in PRCC is defined as

$$|\tilde{\Psi}_0\rangle = e^{T^{(0)}} [1 + \lambda \mathbf{T}^{(1)} \cdot \mathbf{E}_{\text{ext}}] |\Phi_0\rangle, \quad (4)$$

where $\mathbf{T}^{(1)}$ is the perturbed CC operator, and λ is a perturbation parameter. The wavefunction $|\tilde{\Psi}_0\rangle$ is an eigenstate of the modified Hamiltonian $H_{\text{Tot}} = H^{\text{DCB}} - \lambda \mathbf{D} \cdot \mathbf{E}_{\text{ext}}$. The perturbed CC operators $\mathbf{T}^{(1)}$ in Eq. (4) are the solutions of the linearized PRCC equations [21, 22, 24, 25, 33, 34]

$$\langle\Phi_a^p|H_N + [H_N, \mathbf{T}^{(1)}]|\Phi_0\rangle = \langle\Phi_a^p|[\mathbf{D}, T^{(0)}]|\Phi_0\rangle, \quad (5a)$$

$$\langle\Phi_{ab}^{pq}|H_N + [H_N, \mathbf{T}^{(1)}]|\Phi_0\rangle = \langle\Phi_{ab}^{pq}|[\mathbf{D}, T^{(0)}]|\Phi_0\rangle. \quad (5b)$$

where $|\Phi_0\rangle$ is the Dirac-Fock reference wavefunction and $T^{(0)}$ is the closed-shell coupled-cluster (CC) excitation operator. It is an eigenfunction of the Dirac-Coulomb-Breit no-virtual-pair Hamiltonian

$$H^{\text{DCB}} = \sum_{i=1}^N [c\alpha_i \cdot \mathbf{p}_i + (\beta_i - 1)c^2 - V_N(r_i)] + \sum_{i<j} \left[\frac{1}{r_{ij}} + g^{\text{B}}(r_{ij}) \right], \quad (2)$$

where α and β are the Dirac matrices. The negative-energy continuum states of the Hamiltonian are projected out by using the kinetically balanced finite GTO basis sets [29, 30], and selecting only the positive energy states from the finite size basis set [31, 32]. The last two terms, $1/r_{ij}$ and $g^{\text{B}}(r_{ij})$, are the Coulomb and Breit interactions, respectively.

The operators $T^{(0)}$ in Eq. (1) are the solutions of the coupled nonlinear equations

The single and double excitations in the couple-cluster theory capture most of the correlation effects and hence, the operators $T^{(0)}$ and $\mathbf{T}^{(1)}$ are approximated as $T^{(0)} = T_1^{(0)} + T_2^{(0)}$ and $\mathbf{T}^{(1)} = \mathbf{T}_1^{(1)} + \mathbf{T}_2^{(1)}$, respectively. This is referred to as the coupled-cluster single and double (CCSD) approximation [35]. In the present work we, however, also incorporate the triple excitations perturbatively [24].

The perturbed wavefunction from Eq. (4) is used to calculate the ground state polarizability. In PRCC

$$\alpha = - \frac{\langle\tilde{\Psi}_0|\mathbf{D}|\tilde{\Psi}_0\rangle}{\langle\tilde{\Psi}_0|\tilde{\Psi}_0\rangle}. \quad (6)$$

Using the expression of $|\tilde{\Psi}_0\rangle$ from Eq. (4) we can write

$$\alpha = - \frac{\langle\Phi_0|\mathbf{T}^{(1)\dagger} \bar{\mathbf{D}} + \bar{\mathbf{D}} \mathbf{T}^{(1)}|\Phi_0\rangle}{\langle\Psi_0|\Psi_0\rangle}, \quad (7)$$

where $\bar{\mathbf{D}} = e^{T^{(0)\dagger}} \mathbf{D} e^{T^{(0)}}$, and in the denominator $\langle\Psi_0|\Psi_0\rangle$ is the normalization factor. Considering the computational complexity, we truncate $\bar{\mathbf{D}}$ and the normalization factor to second

order in the cluster operators $T^{(0)}$. From our previous study [36], using an iteration scheme we found that the terms with third and higher orders contribute very less to the properties.

III. CALCULATIONAL DETAIL

A. Single-electron basis

In the RCC and PRCC calculations, it is crucial to use an orbital basis set which provides a good description of the single-electron wave functions and energies. In the present work, we use Gaussian-type orbitals (GTOs) [29] as the basis. We optimize the orbitals as well as the self-consistent-field energies of GTOs to match the GRASP2K [37] results. In the Table I, we provide the values of the exponents α_0 and β [29] of the occupied orbital symmetries for Cn, Nh⁺ and Og. For further improvement, we incorporate the effects of Breit interaction, vacuum polarization and the self-energy corrections. This is crucial to obtain the value of the dipole polarizability of SHEs accurately, where the relativistic effects are larger due to higher Z . The effects of finite charge distribution of the nucleus are incorporated using a two-parameter finite size Fermi density distribution.

In the Appendix, we compare the orbital energies of Cn (Table IX), Nh⁺ (Table X) and Og (XI) with GRASP2K [37] and B-spline [38] data. As seen from the tables, the GTOs orbital energies are in excellent agreement with the numerical values from GRASP2K. The largest differences are 3.4×10^{-4} , 4.8×10^{-4} and 9.2×10^{-4} hartree in the case of $4f_{5/2}$, $1s_{1/2}$ and $2p_{1/2}$ orbitals of Cn, Nh⁺ and Og, respectively. The corrections from the vacuum polarization, $\Delta\epsilon_{\text{Ue}}$, and the self-energy, $\Delta\epsilon_{\text{SE}}$, to the orbital energies are provided in the Table XII. Our results match well with the previous calculation [39] for Cn and Og.

B. Computational challenges with SHEs

The calculation of α for SHEs is a computationally challenging task. This is due to the large number of core electrons and the need for larger basis size to obtain converged properties results. The latter pose three main hurdles in the calculations. First, the number of cluster amplitudes is very large, and solving the cluster equations require long compute times. To give an example, as shown in Fig. 1, in the case of Cn using a converge basis of 200 orbitals leads to more than 31 millions cluster amplitudes. This is about 2.3 times larger than the lighter atom Rn. Second, convergence of α with basis size is slow. This is in stark contrast to the convergence trends of α for lighter atoms and ions reported in our previous works [23–25]. For the lighter atoms and ions convergence is achieved with a basis of 160 or less orbitals. However, for SHEs convergence of α requires ≈ 200 orbitals. And third, storing the two-electron integrals for efficient computation require of large memory. For instance, the number of *4-particles* two-electron integrals in the case of Cn is more than 427 millions. This is about 1.3 times larger than the case

of Rn. Moreover, in general parallelization, solving the cluster equations require storing the same set of integrals are stored across all nodes. This leads to replication of data across compute nodes and puts severe restrictions on basis size in the PRCC calculations. To mitigate this problem, we have implemented a *memory-parallel-storage* algorithm [40] which avoids the storage replication of the integrals across different nodes. This allows efficient memory usage and use large orbital basis in the PRCC computations. The inclusion of perturbative triples to the computation of α enhances the computational complexity further. This is due to the evaluation of numerous additional polarizability diagrams arising from the perturbative triples. To illustrate the compute time, the computation of α for Cn using a basis of 200 orbitals without triples takes 120 hrs with 144 threads. Whereas, with partial triples included, it requires 280 hrs with 200 threads. Thus the runtime more than doubled.

IV. RESULTS AND DISCUSSION

A. Convergence of α and correlation energy

Since the GTO basis are mathematically incomplete [32], it is essential to check the convergence of polarizability and correlation energy with basis size. The convergence trends of α and electron correlation energy are shown in the Fig. 2. In these calculations we have used the Dirac-Coulomb Hamiltonian as it is computationally less expensive than using the DCB Hamiltonian. To determine the converged basis set we start with a moderate basis size and add orbitals in each symmetry systematically. This is continued till the change in α and correlation energy is $\leq 10^{-3}$ in their respective units. For example, as discernible from the Table VIII in Appendix, the change in α for Cn is 4.0×10^{-3} a.u. when the basis set is augmented from 191 to 200. So, to optimize the compute time, we consider the basis set with 191 orbitals as the optimal one for α . Once the optimal basis set is chosen, for further computations we incorporate the Breit interaction and QED corrections. As discernible from the Figs. 2(a) and (b), one key observation is, the correlation energies converge with much larger bases than α . For example, for Cn, the converged second-order energy is obtained with the basis size of 439 ($31s27p26d24f22g21h21i21j21k21l$) orbitals. A similar trend is also observed for other two SHEs and all lighter homologs considered in this work.

B. Correlation energy

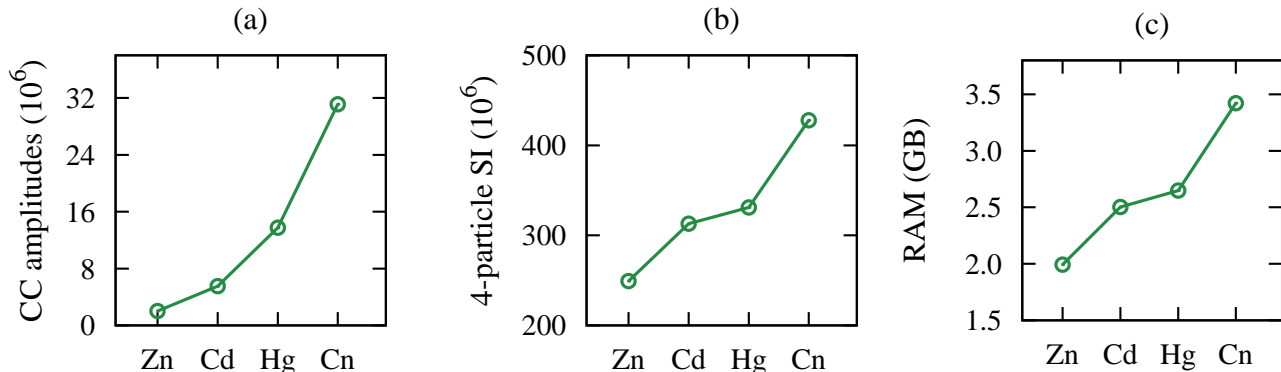
The electron correlation energy in RCC is expressed as

$$\Delta E = \langle \Phi_0 | \tilde{H}_N | \Phi_0 \rangle, \quad (8)$$

where $\tilde{H}_N = e^{-T^{(0)}} H_N e^{T^{(0)}}$, is the similarity transformed Hamiltonian. In Table II, we list ΔE for SHEs and three lighter elements in each group. Since the correlation energies converge with very large basis sizes, it is therefore not practical

TABLE I. The α_0 and β parameters of the even tempered GTO basis used in our calculations.

Atom	s		p		d		f	
	α_0	β	α_0	β	α_0	β	α_0	β
Cn	0.00545	1.870	0.00475	1.952	0.00105	1.970	0.00380	1.965
Og	0.00410	1.910	0.00396	1.963	0.00305	1.925	0.00271	1.830
Nh ⁺	0.05200	1.912	0.03650	1.655	0.05550	1.945	0.00455	1.945

FIG. 1. (a) Number of cluster amplitudes, (b) number of 4-particle Slater integrals and (c) memory required to store 4-particle Slater integrals, as a function of Z for group-12 elements.

to use such a large basis in the RCC calculations due to several computational limitations. Some of the limitations are as mentioned in the previous section. To mitigate this, and to account for correlation energy from the virtuals not included in the RCC calculations, we resort to the second-order MBPT method. The RCC results for ΔE listed in Table II are calculated using the expression

$$\Delta E_{\text{RCC}} \approx \Delta E_{\text{RCC}}^{\text{ncnv}} + \left(\Delta E_{\text{MBPT}}^{\text{conv},2} - \Delta E_{\text{MBPT}}^{\text{ncnv},2} \right), \quad (9)$$

where $\Delta E_{\text{RCC}}^{\text{ncnv}}$ is the correlation energy computed using RCC with orbitals up to j -symmetry. And, $\Delta E_{\text{MBPT}}^{\text{ncnv},2}$ and $\Delta E_{\text{MBPT}}^{\text{conv},2}$ are the second-order energies calculated using RCC basis and a converged basis which includes orbitals up to l -symmetry, respectively.

For all the elements listed in Table II, we observe an important trend in the correlation energy. The RCC energy is smaller in magnitude than the second-order energy. A similar trend is also observed in the previous work [46]. From our calculations we find that the reason for this is the cancellations from the higher order corrections embedded in RCC. As discernible from the Fig. 3(a) for group-12 elements as an example, contributions from the third and fifth order corrections are positive. And, as a result, correlation energy oscillates initially before converging to the RCC value. This can be observed from the Fig. 3(b) where we have shown the cumulative contribution. Comparing our results with previous calculations, to the best of our knowledge, there are no results for SHEs. For lighter elements, our RCC energy agrees well with the previous RCC results [45, 46]. The small difference in the energies, however, could be attributed to the corrections from the Breit and QED included in the present work and the difference in the basis employed. For second-order energies,

there are four results from the previous calculations [41–44]. And, our results match very well with them for all the elements.

Examining the contributions from different symmetries of virtual orbitals, we find that all three SHEs show a similar trend. This is not surprising as all three are closed-shell systems. As discernible from the histograms in Fig. 3, contribution to correlation energy increases initially as a function of orbital symmetry and then decreases. The first two dominant changes, $\approx 35\%$ and 26% of the total correlation energy, are from the g and f orbitals. The next two are from the d and h -symmetries, they contribute $\approx 12\%$ each to all the SHEs. The contribution from the virtuals with l -symmetry is about 0.8% . This non negligible contribution from l -symmetry orbitals indicates that the inclusion of the orbitals from higher symmetries are important to obtain the accurate energies for SHEs.

C. Polarizability

The values of α with different methods subsumed in the PRCC theory are listed in the Table III. The Dirac-Fock (DF) contribution is computed using Eq. (7) with $\mathbf{T}^{(1)}$ and $\bar{\mathbf{D}}$ replaced by the bare dipole operator \mathbf{D} , and is expected to have the dominant contribution. The PRCC values are the converged values from Table VIII, calculated using the DC Hamiltonian with basis up to h symmetry. The values listed as *Estimated* include the estimated contribution from the orbitals of i , j and k symmetries. For this, we use a basis set of moderate size from the Table VIII and then, augment it with orbitals from i , j and k symmetries to calculate percentage contribution, this is added to the PRCC value. To the best of

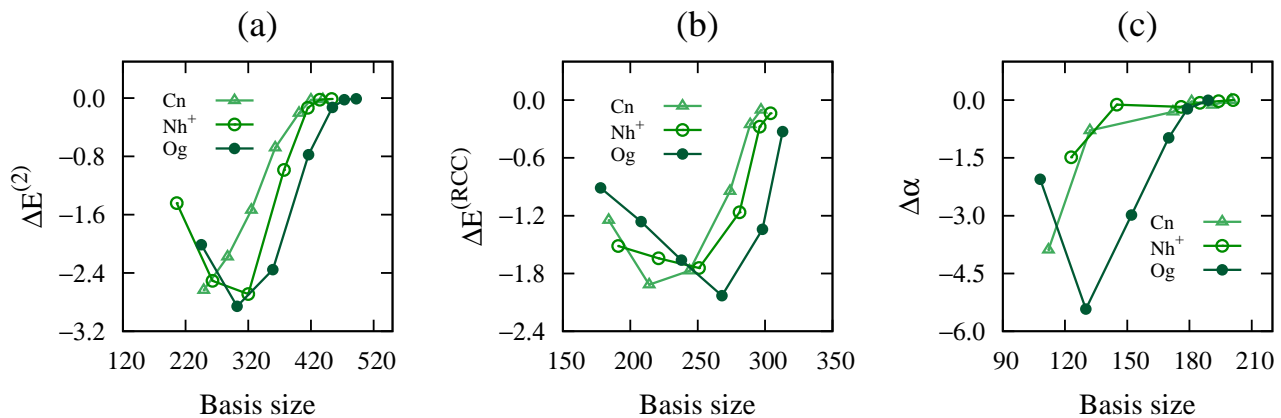


FIG. 2. Convergence of second-order correlation energy (panel (a)), the RCC energy (panel (b)) and α (panel (c)) as function of the basis size.

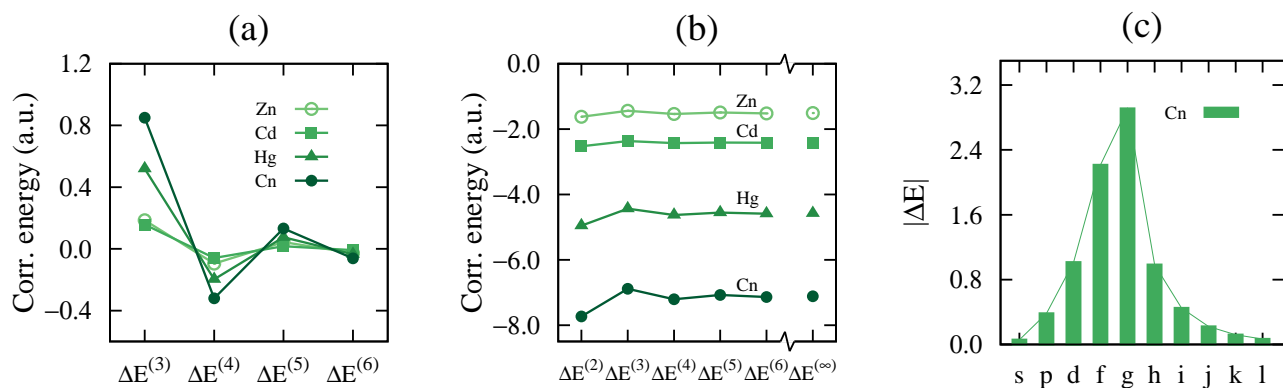


FIG. 3. (a) Third, fourth, fifth and sixth-order correlation energies, (b) cumulative correlation energy and (c) contribution to correlation energy from orbitals of different symmetries. $\Delta E^{(\infty)}$ in panel (b) represents the infinite-order correlation energy and is equivalent to RCC energy.

our knowledge, there are no experimental data on α for SHEs considered in the present work. However, to understand the trend of electron correlation effects, we compare our results with the previous theoretical results. One important and crucial difference between the previous studies and the present work is the absence of QED corrections in the previous works. Though the Breit interaction is included in the previous work [15] for Cn, the contribution is not given explicitly. These corrections are, however, important to obtain the accurate and reliable values of α for SHEs. From our calculations, we find that the combine Breit+QED contributions are $\approx 0.5\%$, 0.4% and 0.6% , respectively, for Cn, Nh⁺ and Og. Considering the important prospects associated with accurate data on α for SHEs, these are significant contributions and can not be neglected.

For Cn three of the previous studies, similar to the present work, are using CCSD(T). There are, however, important differences in terms of the basis used in these calculations. And, this could account for the difference in the values of α reported in these works. In Ref. [15], a relativistic basis with $11s8p8d4f$ orbitals optimized using pseudopotential Hartree-Fock energy is used and reports the smallest value 25.82. The other CCSD(T) result 27.40 from the Ref. [18] is using a rela-

tively larger basis of $26s24p18d13f5g2h$. In terms of methodology and basis, Ref. [18] is the closest to the present work. Our recommended value 27.44(88) is close this. The other CCSD(T) result of 28.68 is from the Ref. [16], which is obtained using an uncontracted Cartesian basis. This is the highest theoretical value reported in the literature. The other value 28 ± 4 is obtained using the RRPA [17]. And, this is close to our result. This is to be expected as both RRPA and PRCC account core-polarization, which is the dominant contribution to α after the DF. For the triples contribution to α , there is no clear trend in the previous RCC results. In Ref. [15] and [18] the contribution from triples reported to as -0.08 and -0.07% of the CCSD value, respectively, and decrease the value of α . However, a positive contribution of $\approx 0.25\%$ is reported in Ref. [16]. In the present work, we obtain a positive contribution of $\approx 1.9\%$, which increases the value of α further.

For Nh⁺, there are no previous theoretical results. The present work reports the first theoretical result of α , using PRCC theory. As we observed from the Table III, though it has the same electronic structure as Cn, the value of α is smaller. This is attributed to the relativistic contraction of $7s_{1/2}$ orbital due to increased nuclear potential. Like the case

TABLE II. Electron correlation and total energies in atomic units for group-12, group-13 and group-18 elements. Listed RCC energies also include the contributions from the Breit and QED corrections.

	Basis		ΔE_{DC}		E_{total}	ΔE_{Others}
	MBPT	RCC	MBPT	RCC		
Group-12						
Zn	336	206	-1.6769	-1.5690	-1796.1812	-1.6975 ^a , -1.6611 ^d -1.6206 ^f
Cd	461	223	-2.7278	-2.6216	-5595.9393	-2.7253 ^b , -2.6540 ^d -2.6500 ^f
Hg	413	227	-5.4681	-5.1164	-19653.9388	-5.4508 ^b , -5.2895 ^d -5.1760 ^f
Cn	439	289	-8.4393	-7.7981	-47335.9752	
Group-13						
Ga ⁺	411	227	-1.669	-1.58077	-1943.9435	
In ⁺	447	235	-2.744	-2.64147	-5882.8838	
Tl ⁺	409	220	-5.499	-5.15772	-20279.7851	
Nh ⁺	453	304	-8.4743	7.8439	-48517.6211	
Group-18						
Kr	413	255	-1.8532	-1.7900	-2790.3898	-1.8907 ^c , -1.8468 ^d -1.8466 ^e -1.8496 ^f
Xe	419	255	-3.0314	-2.9075	-7448.6635	-3.0877 ^c , -2.9587 ^d -2.9979 ^e -3.0002 ^f
Rn	372	245	-5.6195	-5.2945	-23601.3243	-5.7738 ^c , -5.5874 ^d -5.5250 ^f
Og	492	313	-8.9109	-8.3047	-54815.0764	

^aRef.[41][MP2],

^bRef.[42][MP2],

^cRef.[43][MP2],

^dRef.[44][MP2],

^eRef.[45][RCC],

^fRef.[46][RCC],

of Cn, the inclusion of partial triples increases the value of α further.

For Og, there are three previous results based on calculations using CCSD(T). Though the same methods are used, there is a large difference in the values of α reported in these works. For instance, the CCSD(T) value 57.98 reported in Ref. [20] is $\approx 25\%$ larger than the result in Ref. [19]. The reason for this could be attributed to the different types of basis used. In Ref. [19] the computations used the Faegri basis with $26s24p18d13f5g2h$ orbitals, however, in Ref. [20] an uncontracted relativistic quadrupole-zeta basis is used. The other

TABLE III. Final value of α (a. u.) from PRCC calculation compared with other theoretical data in the literature.

Element	Present work		Other cal.
	Method	α	
Cn	DF	35.234	25.82 ^a , 28.68 ^b ,
	PRCC	26.944	27.40 ^d , 28 \pm 4 ^c
	PRCC(T)	27.457	
	PRCC(T)+Breit	27.537	
	PRCC(T)+Breit+QED	27.588	
	Estimated	27.442	
	Recommended	27.44(88)	
Nh ⁺	DF	23.182	
	PRCC	17.056	
	PRCC(T)	17.063	
	PRCC(T)+Breit	17.100	
	PRCC(T)+Breit+QED	17.135	
	Estimated	17.123	
	Recommended	17.12(55)	
Og	DF	56.197	52.43 ^b , 46.33 ^e ,
	PRCC	55.941	57.98 ^f , 57 \pm 3 ^c
	PRCC(T)	56.203	
	PRCC(T)+Breit	56.250	
	PRCC(T)+Breit+QED	56.545	
	Estimated	56.536	
	Recommended	56.54(181)	

^aRef.[15][CCSD(T)],

^bRef.[16][CCSD(T)],

^cRef.[17][RRPA],

^dRef.[18][DC-CCSD(T)],

^eRef.[19][R, DC-CCSD(T)],

^fRef.[20][R, Dirac+Gaunt, CCSD(T)],

TABLE IV. Contributions to α (in a.u.) from different terms in PRCC theory.

Terms + h.c.	Cn	Nh ⁺	Og
$\mathbf{T}_1^{(1)\dagger} \mathbf{D}$	34.5267	21.3767	68.9516
$\mathbf{T}_1^{(1)\dagger} \mathbf{D} \mathbf{T}_2^{(0)}$	-3.0095	-1.7444	-4.0179
$\mathbf{T}_2^{(1)\dagger} \mathbf{D} \mathbf{T}_2^{(0)}$	1.7485	0.7622	3.1900
$\mathbf{T}_1^{(1)\dagger} \mathbf{D} \mathbf{T}_1^{(0)}$	-0.0389	-0.0809	-1.5258
$\mathbf{T}_2^{(1)\dagger} \mathbf{D} \mathbf{T}_1^{(0)}$	-0.1087	-0.0247	0.2319
Normalization	1.2292	1.1898	1.1946
Total	26.9435	17.0524	55.9432

CCSD(T) result 52.43 from Ref. [16] lies between the other two results. Our recommended value 56.54(181) is closer to the RRPA value 57(3) from Ref. [17] and CCSD(T) value, 57.98, from Ref. [20]. As mentioned in the case of Cn, this is due to core-polarization effect accounted to all orders in both CCSD and RRPA. The obtained contribution from partial triples 0.47% is consistent with the contribution 0.66% reported in Ref. [19].

TABLE V. Five leading contribution to $\{\mathbf{T}_1^{(1)\dagger}\mathbf{D} + \text{H.c.}\}$ (in a.u.) for α from core orbitals. This includes the DF and core-polarization contributions.

Cn	Nh ⁺	Og
17.468(7s _{1/2})	11.440(7s _{1/2})	65.874(7p _{3/2})
12.374(6d _{5/2})	6.534(6d _{5/2})	2.392(7p _{1/2})
4.776(6d _{3/2})	3.308(6d _{3/2})	0.562(6d _{5/2})
0.052(6p _{3/2})	0.224(6p _{3/2})	0.264(6d _{3/2})
0.015(5f _{7/2})	0.002(5f _{7/2})	0.042(7s _{1/2})

TABLE VI. Five leading contributions to NLO term $\{\mathbf{T}_1^{(1)\dagger}\mathbf{D}\mathbf{T}_2^{(0)} + \text{H.c.}\}$ (in a.u.) for α from core-core orbital pairs. This includes the pair-correlation contributions.

Cn	Nh ⁺
-0.618(7s _{1/2} , 6d _{5/2})	-0.420(7s _{1/2} , 6d _{5/2})
-0.479(7s _{1/2} , 7s _{1/2})	-0.243(7s _{1/2} , 7s _{1/2})
-0.405(6d _{5/2} , 6d _{5/2})	-0.235(7s _{1/2} , 6d _{3/2})
-0.337(6d _{5/2} , 7s _{1/2})	-0.204(6d _{5/2} , 6d _{5/2})
-0.327(7s _{1/2} , 6d _{3/2})	-0.171(6d _{5/2} , 7s _{1/2})
Og	
-2.805(7p _{3/2} , 7p _{3/2})	
-0.446(7p _{3/2} , 7p _{1/2})	
-0.365(7p _{3/2} , 6d _{5/2})	
-0.167(7p _{3/2} , 6d _{3/2})	
-0.114(7p _{1/2} , 7p _{3/2})	

V. ELECTRON CORRELATION, BREIT AND QED CORRECTIONS

In this section we analyze and present the trends of electron correlation effects from the residual Coulomb interaction, Breit interaction and QED corrections to α as function of Z .

A. Residual Coulomb interaction

To assess the correlation effects from residual Coulomb interaction we define *relative-DF-contribution* (RDFC) as

$$\text{RDFC} = \frac{\alpha_{\text{PRCC}} - \alpha_{\text{DF}}}{\alpha_{\text{DF}}},$$

and plot this for each of the groups in Fig. 4 for all the four elements. As observed from the figure, we obtain similar trends for the group-12 and group-13 elements. For these groups, the RDFC is positive initially and then changes to negative. The reason for this is the drastic change in the nature of the core polarization contribution as function of Z , due to different screening of nuclear potential. The core polarization contribution is positive for first two elements and negative for the last two. This negative contribution reduces the PRCC value to lower than the DF value. A similar trend is also reported

in the previous works [15, 16, 18] where the DF value for Cn is higher than the CCSD value. For the group-18 elements, the RDFC shows a slightly different trend. Except for Kr, it is negative for all the remaining elements. In addition, the magnitude decreases from Xe to Og. This could be attributed to the negative and decreasing core polarization contributions from Xe to Og. Our higher DF value, 56.20, for Og is consistent with the previous results in Refs. [16, 19] in which the reported DF values of 54.46 and 50.01, respectively, are larger than the CCSD values. The difference in the DF values could be due to the different basis used in these calculations, which also led to the different α values.

To gain further insights on the electron correlations effects subsumed in the PRCC theory, we examine the contributions from different terms. And, these are listed in the Table IV. As seen from the table, for all the SHEs, the LO contribution is from the term $\{\mathbf{T}_1^{(1)\dagger}\mathbf{D} + \text{h.c.}\}$. This is to be expected, as it subsumes the contributions from DF and RPA. The contributions are larger than PRCC by $\approx 28\%$, 25% and 23% for Cn, Nh⁺ and Og, respectively. The contribution from the NLO term $\{\mathbf{T}_1^{(1)\dagger}\mathbf{D}\mathbf{T}_2^{(0)}\}$ is small and opposite in phase to the LO term. It accounts for $\approx -11\%$, -10% and -7% of the PRCC value for Cn, Nh⁺ and Og, respectively. The next to NLO (NNLO) term is $\mathbf{T}_2^{(1)\dagger}\mathbf{D}\mathbf{T}_2^{(0)}$ and contributes $\approx 6\%$, 4% and 6% of the PRCC value. The contributions from the other terms are small, and the reason is the smaller magnitude of the $\mathbf{T}_1^{(0)}$ CC operators.

To examine in more detail, we assess the contributions from the core-polarization and pair-correlation effects. For the core-polarization, we identify five dominant contributions to the LO term and these are listed in the Table V. Since the Cn and Nh⁺ have the same ground state electronic configuration, both show similar correlation trends. For both, the most dominant contribution is from the valence orbital 7s_{1/2} and this is due to its larger radial extent. As shown in the Fig. 5, the contribution from 7s_{1/2} is $\approx 50\%$ and 53% of the LO value for Cn and Nh⁺, respectively. For Cn, we find that more than 60% of the 7s_{1/2} contribution arise from $\mathbf{T}_1^{(1)}$ involving the 8p_{1/2}, 10p_{3/2} and 9p_{3/2} orbitals. Whereas for Nh⁺, the 7p_{1/2} and 7p_{3/2} together contribute more than 87% of the total contribution. The next two important contributions are from the core orbitals 6d_{5/2} and 6d_{3/2}. The contribution from the former is almost double of the latter. In particular, for the Cn and Nh⁺ the contributions from 6d_{5/2} is 35% and 30%, respectively. Whereas, the contribution from 6d_{3/2} is $\approx 14\%$ and 15%, respectively. The larger contribution from 6d_{5/2} could be attributed to the strong dipolar mixing with 10p_{3/2} and 9p_{3/2} for Cn, and 7p_{3/2} and 11f_{7/2} for Nh⁺ (see the Fig. 6).

For Og, compare to Cn and Nh⁺, we observe a different trend of core-polarization effect. More than 95% of the contribution from the LO term arises from valence orbital 7p_{3/2}. The other valence and core orbitals contribute less than 5% and 7p_{1/2} contributes only $\approx 3\%$ of the LO term. The reason for this could be the larger radial extent of the 7p_{3/2} orbital as 7p_{1/2} orbital contracts due to relativistic effects. The five dominant contributions arise from the dipolar mixing of 7p_{3/2}

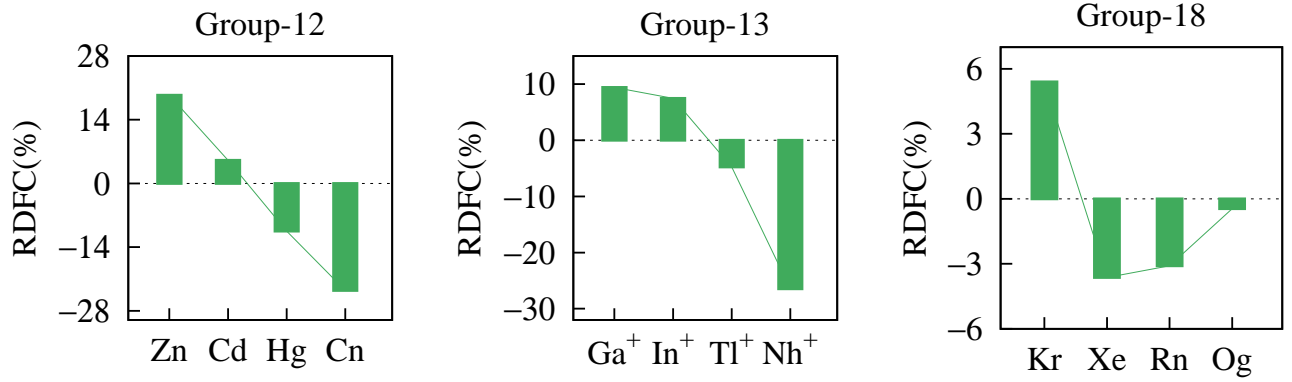


FIG. 4. In percentage, the *relative-DF-contribution* for group-12, group-13 and group-18 elements.

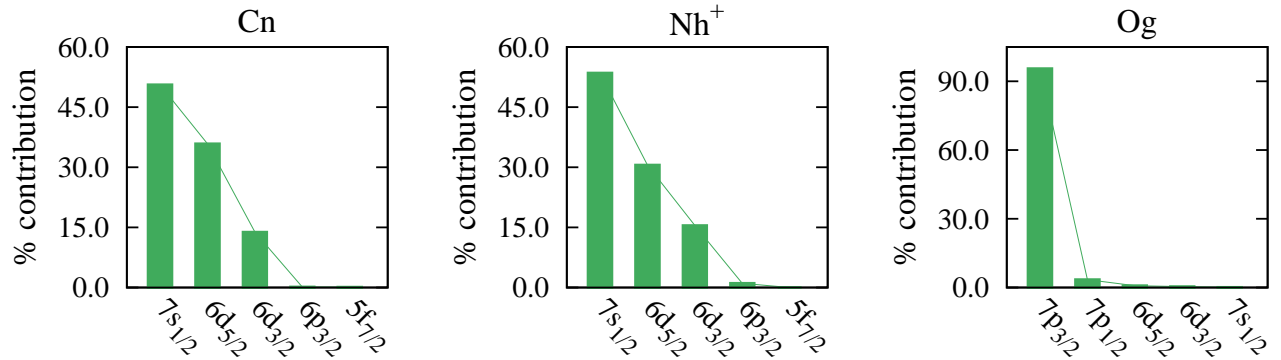


FIG. 5. Five largest percentage contribution from core orbitals to LO term $\{\mathbf{T}_1^{(1)\dagger}\mathbf{D} + \text{h.c.}\}$.

with $10d_{5/2}$, $9d_{5/2}$, $10s_{1/2}$, $9s_{1/2}$ and $11s_{1/2}$ orbitals. These orbitals together contribute $\approx 73\%$ of the total contribution (see the Fig. 6).

To assess the contribution from pair-correlation effects we consider the NLO term and identify the dominant contributions to it. These are listed in the Table VI in terms of the pairs of core orbitals and these correspond to the $T_2^{(0)}$ with dominant contributions. This is an appropriate approach as the most dominant term involving doubly excited cluster operator is the NLO term. For better illustration the percentage contribution to those listed in Table VI are plotted in the Fig. 7. For both Cn and Nh^+ , the first two dominant contributions are from the $(7s_{1/2}, 6d_{5/2})$ and $(7s_{1/2}, 7s_{1/2})$ core-orbital pairs. In percentage, these are $\approx -20\%$ and -16% for Cn, whereas $\approx -24\%$ and -14% for Nh^+ . Though the next three contributions are from the same core-orbital pairs, $(6d_{5/2}, 6d_{5/2})$, $(6d_{5/2}, 7s_{1/2})$ and $(7s_{1/2}, 6d_{3/2})$, in both the elements, there are differences in terms of the order in which they contribute. Like in the core-polarization effect, we observe a different trend for Og. About 70% of the total contribution is from only the $(7p_{3/2}, 7p_{3/2})$ orbital pair.

TABLE VII. Contributions to α from Breit interaction, vacuum polarization and the self-energy corrections in atomic units.

Elements	Z	Breit int.	Self-ene.	Vacuum-pol.
Group-12				
Zn	30	-0.0928	0.0221	-0.0038
Cd	48	-0.0953	0.0648	-0.0159
Hg	80	0.0519	0.0933	-0.0358
Cn	112	0.0802	0.1072	-0.0557
Group-13				
Ga^+	31	-0.3006	0.0090	-0.0018
In^+	49	-0.3647	0.0249	-0.0070
Tl^+	81	-0.1283	0.0526	-0.0274
Nh^+	113	0.0366	0.0794	-0.0440
Group-18				
Kr	36	0.0179	0.0011	0.0009
Xe	54	0.0213	0.0042	0.0031
Rn	86	0.0226	0.0239	0.0181
Og	118	0.0472	0.1162	0.1769

B. Breit and QED corrections

To analyze the trend of correlation effects arising from the Breit interaction, vacuum polarization and the self-energy cor-

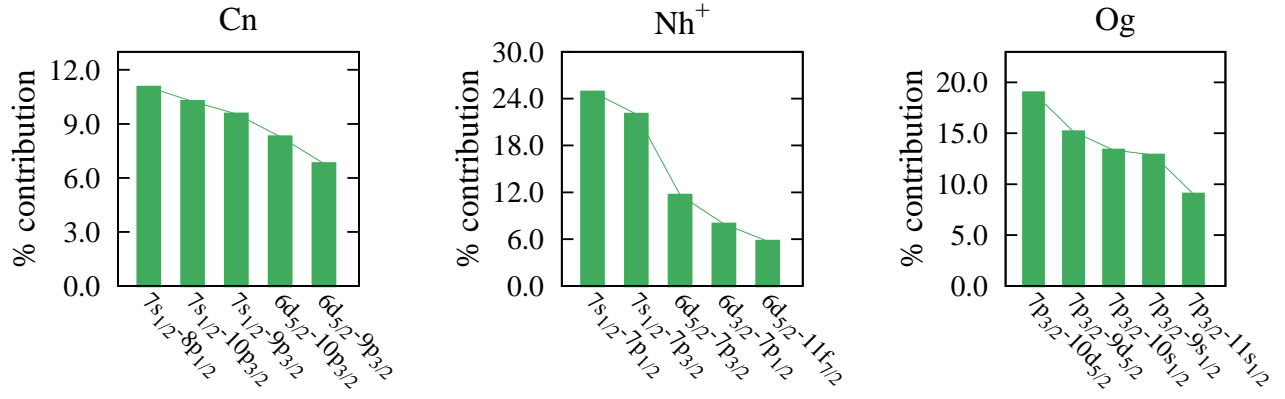


FIG. 6. In percentage, five dominant dipolar mixing of cores with virtuals.

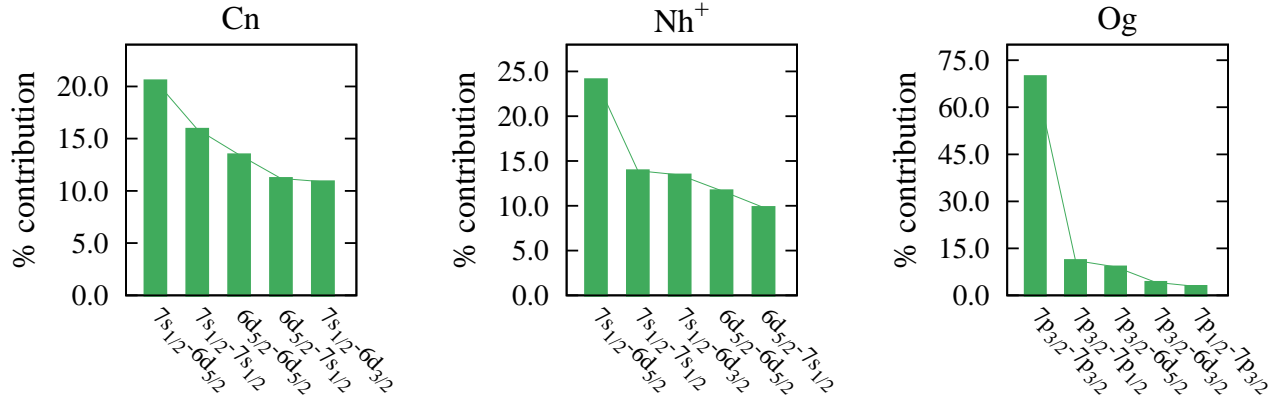


FIG. 7. Five largest percentage contribution from core-core orbital pairs to NLO term.

rections as function of Z , we separate the contributions from these interactions. And, these are listed in the Table VII. In addition, for comparison and to show the trends in the group, the percentage contributions from the corresponding groups in the periodic table of the SHEs are shown in Figs. 8, 9 and 10, respectively. For the Breit interaction, as we see from the Fig. 8, except for the Cn and Og, we observe a trend of decreasing contributions with increasing Z within the groups. One common trend we observe in the contributions to SHEs is that, all are in the same phase as PRCC, and hence increase the value of α . For lighter elements, however, we get a mixed phase for contributions.

For the corrections from the vacuum polarization and self energy, from the Figs. 9 and 10 we see that, the contribution from both the vacuum polarization and self energy increases with Z for all the three groups. This is as expected. For the vacuum polarization, the effect is larger due to higher nuclear charge Z . And, for the self energy, the correction depends on the energy of the orbital, which again depends on the nuclear charge. In terms of the phase of the contributions from vacuum polarization, these are in opposite to PRCC value for all the elements of group-12 and group-13, and hence lowers the value of α . For group-18, however, we observe the contributions of the same phase as PRCC. In terms of magnitude, the

contributions are $\approx 0.21\%$, 0.26% and 0.31% of the PRCC value for Cn, Nh^+ and Og, respectively. For the self energy, one prominent feature of the contributions we observe is that it is positive for all elements in all the three groups, and therefore increase the value of α . The contributions in the case of Cn, Nh^+ and Og are $\approx 0.4\%$, 0.5% and 0.2% of the PRCC value, respectively.

C. Theoretical uncertainty

In this section we discuss the theoretical uncertainty associated with our results for α . For this, we have identified four different sources which can contribute. The first source of uncertainty is the truncation of the basis set in our calculations. The recommended values of α in Table III are obtained from the sum of the converged value with basis up to h -symmetry (see the convergence Table VIII) and the estimated contribution from i , j and k -symmetries. The combine contribution from i , j and k -symmetries are $\approx 0.5\%$, 0.07% and 0.02% , respectively, for Cn, Nh^+ and Og. Though the contributions from the virtuals beyond k -symmetry is expected to be much lower, we select the highest contribution of 0.5% from the case of Cn and attribute this as an upper bound to this source of un-

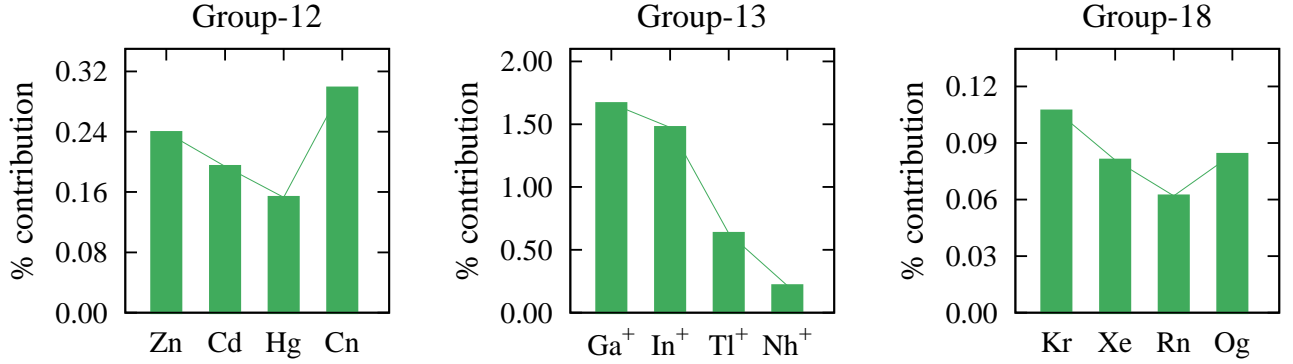


FIG. 8. Percentage contribution from Breit interaction to group-12, group-13 and group-18 elements.

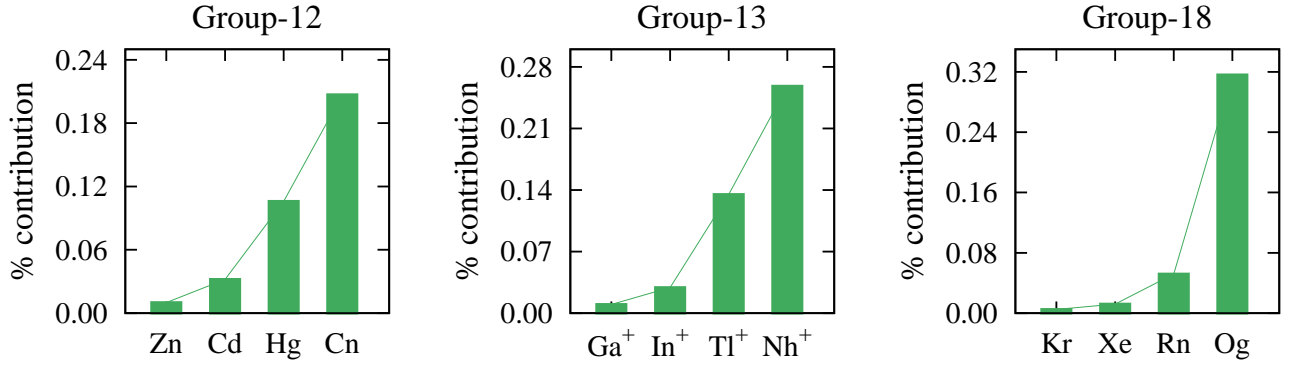


FIG. 9. Percentage contribution from vacuum polarization to group-12, group-13 and group-18 elements.

certainty. The second source is the truncation of the dressed operator $\bar{\mathbf{D}}$ in Eq. (7) to second order in $T^{(0)}$. In our previous work [36], we concluded that the contribution from the remaining higher order terms is less than 0.1%. So, from this source of uncertainty we consider 0.1% as an upper bound. The third source is the partial inclusion of triple excitations in PRCC theory. The partial triples contribute $\approx 1.9\%$, 0.04% , 0.5% of the PRCC value for Cn, Nh^+ and Og, respectively. Since the perturbative triples account for the dominant contribution, we choose the highest contribution of 1.9% from Cn and take it as an upper bound. And, the last source of theoretical uncertainty is associated with the frequency-dependent Breit interaction which is not included in the present work. To estimate an upper bound to from source we use our previous work [23] where using GRASP2K calculations we estimated an upper bound of 0.13% for Ra. Using this with the Breit contributions, we derive $\approx 0.62\%$, 0.45% and 0.18% as the contributions to Cn, Nh^+ and Og, respectively. Among these, we select the highest contribution of 0.62% from the case of Cn and attribute this as an upper bound. There could be other sources of theoretical uncertainty, such as the higher order coupled perturbation of vacuum polarization and self-energy terms, quadruply and higher excited cluster operators, etc. These, however, have much lower contributions and their combined uncertainty could be below 0.1%. Finally, combining the upper bounds of all four sources of uncertainties, we estimate a theoretical uncertainty of 3.2% in the recommended

values of α .

VI. CONCLUSION

We have employed a fully relativistic coupled-cluster theory to compute the ground state electric dipole polarizability and electron correlation energy of SHEs Cn, Nh^+ and Og. In addition, to understand the trend of electron correlation as function of Z , we have calculated the correlation energies of three lighter homologs for each SHEs. To improve the accuracy of our results, contributions from the Breit interaction, QED corrections and partial triple excitations are also included. Moreover, in all calculations, very large bases up to l -symmetry are used to check the convergence of the results.

Our recommended values of α for SHEs lie between the previous results, more closer to the values from CCSD(T) [18, 20] and RPA [17] calculations. From our calculations we find that the dominant contribution to α comes from the valence electrons, viz, $7s_{1/2}$ for both Cn and Nh^+ , and $7p_{3/2}$ for Og. While $7s_{1/2}$ contributes more than 50% of the total value for Cn and Nh^+ , the contribution from $7p_{3/2}$ orbital to Og is more than 95%. This could be attributed to the larger radial extent of these orbitals.

From the analysis of electron correlation effects, we find that, for all three groups, the core polarization contribution decreases as function of Z for the lighter homologs. For SHEs,

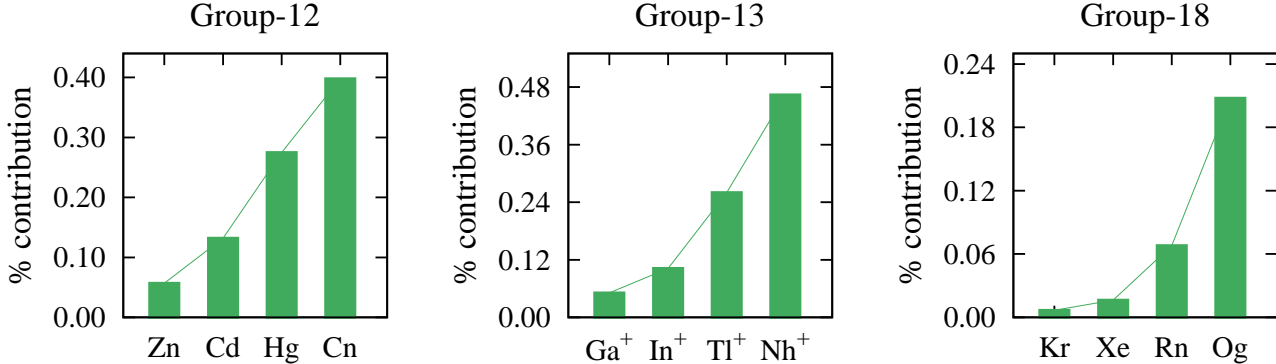


FIG. 10. Percentage contribution from self-energy correction to group-12, group-13 and group-18 elements.

however, we observed an increased contribution, of the order of the first element considered in each group. For the corrections from the Breit interaction, except for Cn and Og, a trend of decreasing contributions as function of Z is observed. On contrary, for Uehling potential and the self-energy corrections, we observed a trend of increasing contributions from lighter homologs to SHEs. The largest contributions from the Uehling potential are $\approx 0.2\%$, 0.3% and 0.3% of PRCC value for Cn, Nh⁺ and Og, respectively. And, the same from the self-energy corrections are $\approx 0.4\%$, 0.2% and 0.1% , respectively. The combined Breit+QED corrections to α are observed to be $\approx 0.5\%$, 0.4% and 0.6% for Cn, Nh⁺ and Og, respectively. Considering the importance of accurate properties results of SHEs, these are significant contributions, and can not be neglected.

We report the first result on the electron correlation energy for SHEs Cn, Nh⁺ and Og using RCC. From our detailed analysis on correlation energy, we find that the second-order MBPT calculations overestimate the electron correlation energy for all superheavy elements and lighter homologs considered in this work.

ACKNOWLEDGMENTS

We would like to thank Chandan Kumar Vishwakarma for useful discussions. One of the authors, BKM, acknowledges the funding support from the SERB (ECR/2016/001454). The results presented in the paper are based on the computations using the High Performance Computing cluster, Padum, at the Indian Institute of Technology Delhi, New Delhi.

Appendix A: Convergence table for α

In Table VIII we provide the convergence trend of α as function of basis size. As it is evident from the table, the value of α converges to 10^{-3} a.u. for all three SHEs.

TABLE VIII. Convergence trend of α calculated using the Dirac-Coulomb Hamiltonian as a function of basis size.

Basis	Orbitals	α
Cn		
90	14s, 11p, 10d, 8f, 6g, 3h	32.772
112	16s, 13p, 12d, 10f, 8g, 5h	28.884
132	18s, 15p, 14d, 12f, 9g, 7h	28.094
152	20s, 17p, 16d, 14f, 11g, 8h	27.418
172	22s, 19p, 18d, 16f, 13g, 9h	27.116
181	23s, 20p, 19d, 17f, 14g, 9h	27.078
191	25s, 21p, 20d, 18f, 15g, 9h	26.948
200	26s, 22p, 21d, 19f, 16g, 9h	26.944
Nh ⁺		
101	15s, 13p, 12d, 8f, 5g, 5h	19.493
123	17s, 15p, 14d, 10f, 7g, 7h	18.009
145	19s, 17p, 16d, 12f, 9g, 9h	17.889
167	21s, 19p, 18d, 14f, 11g, 11h	17.330
176	22s, 20p, 19d, 15f, 12g, 11h	17.155
185	23s, 21p, 20d, 16f, 13g, 11h	17.082
194	24s, 22p, 21d, 17f, 14g, 11h	17.053
201	25s, 23p, 22d, 18f, 14g, 11h	17.053
Og		
86	14s, 12p, 9d, 7f, 5g, 3h	67.613
108	16s, 14p, 11d, 9f, 7g, 5h	65.556
130	18s, 16p, 13d, 11f, 9g, 7h	60.134
152	20s, 18p, 15d, 13f, 11g, 9h	57.149
170	22s, 20p, 17d, 15f, 12g, 10h	56.170
179	23s, 21p, 18d, 16f, 13g, 10h	55.943
189	25s, 22p, 19d, 17f, 14g, 10h	55.941

Appendix B: Single-electron energies

The single-electron energies of GTOs for SHEs Cn, Nh⁺ and Og are listed in the Tables IX, X and XI, respectively, and compared with the numerical data from GRASP2k [37] and

the energies from the B-spline [] basis. In Table XII, we list the contributions from the Breit interaction, Uehling potential and the self-energy corrections to the single-electron energies.

TABLE IX. Orbital energies for core orbitals (in Hartree) from GTO is compared with the GRASP2K and B-spline energies for Cn. Here [x] represents multiplication by 10^x .

Orbital	GRASP2K	B-spline	GTO
$1s_{1/2}$	7070.83320	7071.11186	7070.83326
$2s_{1/2}$	1444.87110	1444.92899	1444.87138
$3s_{1/2}$	390.81374	390.82783	390.81406
$4s_{1/2}$	113.44660	113.45069	113.44692
$5s_{1/2}$	30.05645	30.05764	30.05670
$6s_{1/2}$	5.68070	5.68099	5.68070
$7s_{1/2}$	0.45115	0.45119	0.45114
$2p_{1/2}$	1405.71950	1405.72953	1405.71920
$3p_{1/2}$	371.98098	371.98361	371.98109
$4p_{1/2}$	104.23703	104.23780	104.23723
$5p_{1/2}$	25.88719	25.88738	25.88726
$6p_{1/2}$	4.12316	4.12320	4.12312
$2p_{3/2}$	1007.09780	1007.09651	1007.09804
$3p_{3/2}$	274.99360	274.99302	274.99388
$4p_{3/2}$	76.37753	76.37735	76.37776
$5p_{3/2}$	17.99726	17.99719	17.99718
$6p_{3/2}$	2.41564	2.41562	2.41564
$3d_{3/2}$	245.88774	245.88719	245.88802
$4d_{3/2}$	62.08615	62.08599	62.08641
$5d_{3/2}$	11.85266	11.85260	11.85259
$6d_{3/2}$	0.56273	0.56271	0.56273
$3d_{5/2}$	229.40040	229.39991	229.40069
$4d_{5/2}$	57.56171	57.56155	57.56196
$5d_{5/2}$	10.70702	10.70697	10.70692
$6d_{5/2}$	0.44208	0.44207	0.44208
$4f_{5/2}$	38.82989	38.82975	38.83023
$5f_{5/2}$	3.33495	3.33492	3.33493
$4f_{7/2}$	37.51594	37.51581	37.51628
$5f_{7/2}$	3.09251	3.09247	3.09248

-
- [1] Andreas Türler and Valeria Pershina, “Advances in the production and chemistry of the heaviest elements,” *Chemical Reviews* **113**, 1237–1312 (2013), pMID: 23402305, <https://doi.org/10.1021/cr3002438>.
- [2] Matthias Schädel, “Chemistry of the superheavy elements,” *Philosophical Transactions of the Royal Society A: Mathematical, Physical and Engineering Sciences*, **373**, 20140191 (2015), <https://royalsocietypublishing.org/doi/pdf/10.1098/rsta.2014.0191>.
- [3] V. Pershina, “Electronic structure and properties of superheavy elements,” *Nuclear Physics A* **944**, 578 – 613 (2015), special Issue on Superheavy Elements.
- [4] Peter Schwerdtfeger, Lukáš F. Pašteka, Andrew Punnett, and Patrick O. Bowman, “Relativistic and quantum electrodynamic effects in superheavy elements,” *Nuclear Physics A* **944**, 551 – 577 (2015), special Issue on Superheavy Elements.
- [5] Ephraim Eliav, Stephan Fritzsche, and Uzi Kaldor, “Electronic structure theory of the superheavy elements,” *Nuclear Physics A* **944**, 518 – 550 (2015), special Issue on Superheavy Elements.
- [6] S. A. Giuliani, Z. Matheson, W. Nazarewicz, E. Olsen, P.-G. Reinhard, and the SLLS team, *Phys. Rev. Lett.* **111**, 202501 (2013), <https://doi.org/10.1103/PhysRevLett.111.202501>.
- [7] D. Shaughnessy and M. Schadel, *The Chemistry of the Superheavy Elements*, 2nd ed. (Springer, Heidelberg, 2014).
- [8] V. Pershina and D.C. Hoffman, *Transactinide Elements and Future Elements* (Springer, Dordrecht, 2008).
- [9] I.B. Khriplovich, *Parity Nonconservation in Atomic Phenomena* (Gordon and Breach Science Publishers, Philadelphia, 1991).

TABLE X. Orbital energies for core orbitals (in Hartree) from GTO is compared with the GRASP2K and B-spline energies for Nh⁺. Here [x] represents multiplication by 10^x.

Orbital	GRASP2K	B-spline	GTO
1s _{1/2}	7245.8727391	7246.182976	7245.873218
2s _{1/2}	1487.4479289	1487.512728	1487.448327
3s _{1/2}	403.5128636	403.529178	403.513164
4s _{1/2}	117.9615376	117.966271	117.961704
5s _{1/2}	31.8304473	31.831827	31.830498
6s _{1/2}	6.4543326	6.454659	6.454278
7s _{1/2}	0.8293919	0.829453	0.829389
2p _{1/2}	1448.2662707	1448.277353	1448.266677
3p _{1/2}	384.4936370	384.497093	384.493911
4p _{1/2}	108.6076330	108.608617	108.607744
5p _{1/2}	27.5681904	27.568442	27.568231
6p _{1/2}	4.8384890	4.838538	4.838465
2p _{3/2}	1028.6629340	1028.661537	1028.663316
3p _{3/2}	282.2280516	282.227605	282.228310
4p _{3/2}	79.1393402	79.139197	79.139459
5p _{3/2}	19.1605082	19.160449	19.160489
6p _{3/2}	2.9774011	2.977385	2.977406
3d _{3/2}	252.7000748	252.699678	252.700378
4d _{3/2}	64.6075721	64.607451	64.607745
5d _{3/2}	12.8763169	12.876269	12.876364
6d _{3/2}	1.0204591	1.020450	1.020479
3d _{5/2}	235.5220171	235.521671	235.522311
4d _{5/2}	59.8711971	59.871089	59.871368
5d _{5/2}	11.6644138	11.664335	11.664411
6d _{5/2}	0.8811957	0.881171	0.881195
4f _{5/2}	40.8372335	40.837027	40.837249
5f _{5/2}	4.0945793	4.094568	4.094589
4f _{7/2}	39.4570885	39.456886	39.457103
5f _{7/2}	3.8335434	3.833539	3.833556

TABLE XI. Orbital energies for core orbitals (in Hartree) from GTO is compared with the GRASP2K and B-spline energies for Og. Here [x] represents multiplication by 10^x.

Orbital	GRASP2K	B-spline	GTO
1s _{1/2}	8185.36230	8185.93230	8185.36258
2s _{1/2}	1718.80780	1718.93698	1718.80803
3s _{1/2}	471.19401	471.22553	471.19411
4s _{1/2}	140.97641	140.98548	140.97632
5s _{1/2}	39.88519	39.88767	39.88495
6s _{1/2}	8.98686	8.98760	8.98678
7s _{1/2}	1.29699	1.29711	1.29696
2p _{1/2}	1681.71710	1681.74523	1681.71618
3p _{1/2}	451.72699	451.73439	451.72665
4p _{1/2}	131.02105	131.02303	131.02069
5p _{1/2}	35.18375	35.18404	35.18340
6p _{1/2}	7.07694	7.07713	7.07689
7p _{1/2}	0.73956	0.73948	0.73944
2p _{3/2}	113.85447	1138.54073	1138.54500
3p _{3/2}	318.33517	318.33345	318.33518
4p _{3/2}	92.02425	92.02349	92.02406
5p _{3/2}	23.66280	23.66234	23.66242
6p _{3/2}	4.21643	4.21630	4.21633
7p _{3/2}	0.30564	0.30564	0.30565
3d _{3/2}	286.65027	286.64895	286.65036
4d _{3/2}	76.26542	76.26467	76.26535
5d _{3/2}	16.66319	16.66277	16.66297
6d _{3/2}	1.76398	1.76387	1.76394
3d _{5/2}	265.67617	265.67496	265.67625
4d _{5/2}	70.35026	70.34956	70.35019
5d _{5/2}	15.07066	15.07028	15.07044
6d _{5/2}	1.49296	1.49285	1.49291
4f _{5/2}	49.79167	49.79139	49.79205
5f _{5/2}	6.51102	6.51097	6.51114
4f _{7/2}	48.04247	48.04220	48.04286
5f _{7/2}	6.14074	6.14070	6.14086

- [10] W. C. Griffith, M. D. Swallows, T. H. Loftus, M. V. Romalis, B. R. Heckel, and E. N. Fortson, “Improved limit on the permanent electric dipole moment of Hg¹⁹⁹,” *Phys. Rev. Lett.* **102**, 101601 (2009).
- [11] Th. Udem, R. Holzwarth, and T. W. Hansch, “Optical frequency metrology,” *Nature* **416**, 233 (2002).
- [12] M. Lewenstein, Ph. Balcou, M. Yu. Ivanov, Anne L’Huillier, and P. B. Corkum, “Theory of high-harmonic generation by low-frequency laser fields,” *Phys. Rev. A* **49**, 2117–2132 (1994).
- [13] M. H. Anderson, J. R. Ensher, M. R. Matthews, C. E. Wieman, and E. A. Cornell, “Observation of Bose-Einstein condensation in a dilute atomic vapor,” *Science* **269**, 198–201 (1995).
- [14] S. G. Karshenboim and E. Peik, *Astrophysics, Clocks and Fundamental Constants, Lecture Notes in Physics* (Springer, New York, 2010).
- [15] Michael Seth, Peter Schwerdtfeger, and Michael Dolg, “The chemistry of the superheavy elements. i. pseudopotentials for 111 and 112 and relativistic coupled cluster calculations for (112)h+, (112)f2, and (112)f4,” *The Journal of Chemical Physics* **106**, 3623–3632 (1997), <https://doi.org/10.1063/1.473437>.
- [16] Clinton S. Nash, “Atomic and molecular properties of elements 112, 114, and 118,” *The Journal of Physical Chemistry A* **109**, 3493–3500 (2005), pMID: 16833687, <https://doi.org/10.1021/jp050736o>.
- [17] V. A. Dzuba, “Ionization potentials and polarizabilities of superheavy elements from Db to Cn (Z=105–112),” *Phys. Rev. A* **93**, 032519 (2016).
- [18] V. Pershina, A. Borschevsky, E. Eliav, and U. Kaldor, “Prediction of the adsorption behavior of elements 112 and 114 on inert surfaces from ab initio dirac-coulomb atomic calculations,” *The Journal of Chemical Physics* **128**, 024707 (2008), <https://doi.org/10.1063/1.2814242>.
- [19] V. Pershina, A. Borschevsky, E. Eliav, and U. Kaldor, “Adsorption of inert gases including element 118 on noble metal and inert surfaces from ab initio dirac-coulomb atomic calculations,” *The Journal of Chemical Physics* **129**, 144106 (2008), <https://doi.org/10.1063/1.2988318>.
- [20] Paul Jerabek, Bastian Schuettrumpf, Peter Schwerdtfeger, and Witold Nazarewicz, “Electron and nucleon localization functions of oganesson: Approaching the thomas-fermi limit,” *Phys. Rev. Lett.* **120**, 053001 (2018).
- [21] S. Chattopadhyay, B. K. Mani, and D. Angom, “Perturbed coupled-cluster theory to calculate dipole polarizabilities of closed-shell systems: Application to ar, kr, xe, and rn,”

- Phys. Rev. A **86**, 062508 (2012).
- [22] S. Chattopadhyay, B. K. Mani, and D. Angom, “Electric dipole polarizabilities of doubly ionized alkaline-earth-metal ions from perturbed relativistic coupled-cluster theory,” *Phys. Rev. A* **87**, 062504 (2013).
- [23] S. Chattopadhyay, B. K. Mani, and D. Angom, “Electric dipole polarizability of alkaline-earth-metal atoms from perturbed relativistic coupled-cluster theory with triples,” *Phys. Rev. A* **89**, 022506 (2014).
- [24] S. Chattopadhyay, B. K. Mani, and D. Angom, “Triple excitations in perturbed relativistic coupled-cluster theory and electric dipole polarizability of group-ii elements,” *Phys. Rev. A* **91**, 052504 (2015).
- [25] Ravi Kumar, S. Chattopadhyay, B. K. Mani, and D. Angom, “Electric dipole polarizability of group-13 ions using perturbed relativistic coupled-cluster theory: Importance of non-linear terms,” *Phys. Rev. A* **101**, 012503 (2020).
- [26] M. S. Safronova, W. R. Johnson, and A. Derevianko, “Relativistic many-body calculations of energy levels, hyperfine constants, electric-dipole matrix elements, and static polarizabilities for alkali-metal atoms,” *Phys. Rev. A* **60**, 4476–4487 (1999).
- [27] A. Derevianko, W. R. Johnson, M. S. Safronova, and J. F. Babb, “High-precision calculations of dispersion coefficients, static dipole polarizabilities, and atom-wall interaction constants for alkali-metal atoms,” *Phys. Rev. Lett.* **82**, 3589–3592 (1999).
- [28] J. Sucher, “Foundations of the relativistic theory of many-electron atoms,” *Phys. Rev. A* **22**, 348–362 (1980).
- [29] A. K. Mohanty, F. A. Parpia, and E. Clementi, “Kinetically balanced geometric gaussian basis set calculations for relativistic many-electron atoms,” in *Modern Techniques in Computational Chemistry: MOTEC-91*, edited by E. Clementi (ES-COM, 1991).
- [30] Richard E. Stanton and Stephen Havriliak, “Kinetic balance: A partial solution to the problem of variational safety in dirac calculations,” *J. Chem. Phys.* **81**, 1910–1918 (1984).
- [31] I. P. Grant, *Relativistic Quantum Theory of Atoms and Molecules: Theory and Computation* (Springer, New York, 2010).
- [32] Ian Grant, “Relativistic atomic structure,” in *Springer Handbook of Atomic, Molecular, and Optical Physics*, edited by Gordon Drake (Springer, New York, 2006) pp. 325–357.
- [33] S. Chattopadhyay, B. K. Mani, and D. Angom, “Electric dipole polarizability from perturbed relativistic coupled-cluster theory: Application to neon,” *Phys. Rev. A* **86**, 022522 (2012).
- [34] S. Chattopadhyay, B. K. Mani, and D. Angom, “Electric dipole polarizabilities of alkali-metal ions from perturbed relativistic coupled-cluster theory,” *Phys. Rev. A* **87**, 042520 (2013).
- [35] George D. Purvis and Rodney J. Bartlett, “A full coupled-cluster singles and doubles model: The inclusion of disconnected triples,” *J. Chem. Phys.* **76**, 1910–1918 (1982).
- [36] B. K. Mani and D. Angom, “Atomic properties calculated by relativistic coupled-cluster theory without truncation: Hyperfine constants of mg^+ , ca^+ , sr^+ , and ba^+ ,” *Phys. Rev. A* **81**, 042514 (2010).
- [37] P. Jönsson, G. Gaigalas, J. Bieroń, C. Froese Fischer, and I. P. Grant, “New version: Grasp2k relativistic atomic structure package,” *Comp. Phys. Comm.* **184**, 2197 – 2203 (2013).
- [38] Oleg Zatsarinny and Charlotte Froese Fischer, “DBSR-HF: A B-spline Dirac–Hartree–Fock program,” *Computer Physics Communications* **202**, 287 – 303 (2016).
- [39] Karol Koziol and Gustavo A. Aucar, “Qed effects on individual atomic orbital energies,” *The Journal of Chemical Physics* **148**, 134101 (2018), <https://doi.org/10.1063/1.5026193>.
- [40] B.K. Mani, S. Chattopadhyay, and D. Angom, “Rccpac: A parallel relativistic coupled-cluster program for closed-shell and one-valence atoms and ions in fortran,” *Computer Physics Communications* **213**, 136 – 154 (2017).
- [41] J R Flores and P Redondo, “Computation of second-order correlation energies using a finite element method for atoms with d electrons,” *Journal of Physics B: Atomic, Molecular and Optical Physics* **26**, 2251–2261 (1993).
- [42] Jesús R. Flores and P. Redondo, “High-precision atomic computations from finite element techniques: Second-order correlation energies for be, ca, sr, cd, ba, yb, and hg,” *Journal of Computational Chemistry* **15**, 782–790 (1994), <https://onlinelibrary.wiley.com/doi/pdf/10.1002/jcc.540150710>.
- [43] Jesús R. Flores, “High precision atomic computations from finite element techniques: Second-order correlation energies of rare gas atoms,” *The Journal of Chemical Physics* **98**, 5642–5647 (1993), <https://doi.org/10.1063/1.464908>.
- [44] Yasuyuki Ishikawa and Konrad Koc, “Relativistic many-body perturbation theory based on the no-pair Dirac–Coulomb–Breit Hamiltonian: Relativistic correlation energies for the noble-gas sequence through Rn ($Z=86$), the group-ii atoms through Hg, and the ions of Ne isoelectronic sequence,” *Phys. Rev. A* **50**, 4733–4742 (1994).
- [45] B. K. Mani, K. V. P. Latha, and D. Angom, “Relativistic coupled-cluster calculations of ^{20}Ne , ^{40}Ar , ^{84}Kr , and ^{129}Xe : Correlation energies and dipole polarizabilities,” *Phys. Rev. A* **80**, 062505 (2009).
- [46] Shane P. McCarthy and Ajit J. Thakkar, “Accurate all-electron correlation energies for the closed-shell atoms from Ar to Rn and their relationship to the corresponding MP2 correlation energies,” *The Journal of Chemical Physics* **134**, 044102 (2011), <https://doi.org/10.1063/1.3547262>.

TABLE XII. The orbital energies for core orbitals from vacuum polarization and self energy correction for Cn, Nh⁺ and Og.

Orbital	Cn				Nh ⁺		Og			
	$\Delta\epsilon_{Ue}$		$\Delta\epsilon_{SE}$		$\Delta\epsilon_{Ue}$	$\Delta\epsilon_{SE}$	$\Delta\epsilon_{Ue}$		$\Delta\epsilon_{SE}$	
	Ours	Ref. [39]	Ours	Ref. [39]	Ours	Ours	Ours	Ref. [39]	Ours	Ref. [39]
1s _{1/2}	-11.1193	-11.4416	30.6243	30.5752	-11.8402	31.9902	-16.2622	-16.7082	39.9045	39.7825
2s _{1/2}	-2.1505	-2.2283	5.9196	5.7672	-2.3160	6.2339	-3.3693	-3.4810	8.1051	7.7743
3s _{1/2}	-0.5193	-0.5410	1.4424	1.5061	-0.5597	1.5198	-0.8134	-0.8487	1.9781	2.1609
4s _{1/2}	-0.1494	-0.1560	0.4165	0.4375	-0.1614	0.4400	-0.2377	-0.2482	0.5795	0.6369
5s _{1/2}	-0.0436		0.1214		-0.0474	0.1291	-0.0718		0.1783	
6s _{1/2}	-0.0108		0.0297		-0.0119	0.0322	-0.0197		0.0500	
7s _{1/2}	-0.0015		0.0037		-0.0019	0.0047	-0.0040		0.0098	
2p _{1/2}	-0.5505	-0.6632	1.6011	1.6611	-0.6457	1.7455	-1.0858	-1.2661	2.7124	2.7853
3p _{1/2}	-0.1486	-0.1801	0.4445	0.5091	-0.1662	0.4835	-0.2926	-0.3430	0.7399	0.8812
4p _{1/2}	-0.0422	-0.0523	0.1278	0.1551	-0.0473	0.1394	-0.0845	-0.1010	0.2156	0.2712
5p _{1/2}	-0.0115		0.0359		-0.0130	0.0395	-0.0242		0.0674	
6p _{1/2}	-0.0024		0.0080		-0.0028	0.0090	-0.0059		0.0177	
7p _{1/2}							-0.0010		0.0027	
2p _{3/2}	0.0554	-0.0122	0.6914	0.6997	0.0594	0.7207	0.0848	-0.0169	0.8799	0.9013
3p _{3/2}	0.0183	-0.0038	0.1896	0.2002	0.0197	0.1983	0.0287	-0.0054	0.2476	0.2644
4p _{3/2}	0.0068	-0.0011	0.0565	0.0613	0.0074	0.0594	0.0110	-0.0017	0.0774	0.0827
5p _{3/2}	0.0026		0.0157		0.0028	0.0167	0.0043		0.0224	
6p _{3/2}	0.0009		0.0029		0.0010	0.0032	0.0016		0.0046	
7p _{3/2}								0.0003	0.0005	0.0445
3d _{3/2}	0.0205	-0.0001	-0.0015	-0.0014	0.0221	-0.0012	0.0316	-0.0002	0.0012	0.0012
4d _{3/2}	0.0070	0	-0.0005	0.0009	0.0076	-0.0004	0.0112	-0.0001	0.0004	0.0023
5d _{3/2}	0.0024		-0.0001		0.0026	-0.0001	0.0040		0.0001	
6d _{3/2}	0.0007		0		0.0007	0	0.0011		0	
3d _{5/2}	0.0185	0	0.0253	0.0231	0.0199	0.0265	0.0282	0	0.0333	0.0304
4d _{5/2}	0.0064	0	0.0084	0.0064	0.0069	0.0089	0.0102	0	0.0115	0.0086
5d _{5/2}	0.0022		0.0024		0.0024	0.0023	0.0036		0.0031	
6d _{5/2}	0.0006		0.0002		0.0006	0.0003	0.0010		0.0005	
4f _{5/2}	0.0055				0.0059		0.0088			
5f _{5/2}	0.0015				0.0017		0.0027			
4f _{7/2}	0.0053				0.0057		0.0084			
5f _{7/2}	0.0015				0.0016		0.0026			